International Journal of Nanomedicine Dovepress

Open Access Full Text Article ORIGINAL RESEARCH

Regenerative Potential Nanomedicine of Adipocyte Stem Cell-Derived Exosomes in Senescent Skin Tissue

An-Na Li[1,*], Jing-Hua Sun[1,2,*], Syafiqah Saidin[3,4], Jee Syuen Cheah[4,5], Chia-Hung Kuo[6], Ling Li[1], Jia-Shen Li[1], Ru-Yu Bai[1], Yong Diao[1], Hui-Min David Wang[5,7–9]

[1]School of Medicine, Huaqiao University, Quanzhou, Fujian, 362021, People's Republic of China; [2]Hebei Key Laboratory of Basic Medicine for Diabetes, Shijiazhuang Second Hospital, Shijiazhuang, Hebei, 050000, People's Republic of China; [3]IJN-UTM Cardiovascular Engineering Centre, Institute of Human Centered Engineering, Universiti Teknologi Malaysia, Johor Bahru, Johor, 81310, Malaysia; [4]Department of Biomedical Engineering & Health Sciences, Faculty of Electrical Engineering, Universiti Teknologi Malaysia, Johor Bahru, Johor, 81310, Malaysia; [5]Graduate Institute of Biomedical Engineering, National Chung Hsing University, Taichung, Taiwan, Republic of China; [6]Department of Seafood Science, National Kaohsiung University of Science and Technology, Kaohsiung, Taiwan, Republic of China; [7]Regenerative Medicine and Cell Therapy Research Center; and Graduate Institute of Medicine, College of Medicine, Kaohsiung Medical University, Kaohsiung, Taiwan, Republic of China; [8]Department of Medical Laboratory Science and Biotechnology, China Medical University, Taichung, Taiwan, Republic of China; [9]Center of Applied Nanomedicine, National Cheng Kung University, Tainan, Taiwan, Republic of China

*These authors contributed equally to this work

Correspondence: Hui-Min David Wang, Graduate Institute of Biomedical Engineering, National Chung Hsing University, No. 145, Xingda Road, South District, Taichung City, 402, Taiwan, Republic of China, Tel +886 4 22840733 #651; +886 935753718, Email davidw@dragon.nchu.edu.tw; Yong Diao, School of Medicine, Huaqiao University, Quanzhou, Fujian, 362021, People's Republic of China, Email diaoyong@hqu.edu.cn

Introduction: Skin is the first-line barrier defense against infection, irradiation, and toxins, but is prone to natural aging (intrinsic aging) and environmental factors (extrinsic aging). Hence, there is an increasing urgency to explore an effective treatment for aging skin. This study was focused on testing the potential of utilizing adipocyte stem cell derived exosomal as nanomedicine to regenerate the dermal layer and counteract signs of skin aging.

Methods: The harvested stem cells from adipose tissues were isolated, cultured, and then starved. The centrifugation of cell cultures medium yielded the human adipose-derived stem cells conditional medium (HADSCs-CM). Collagen secretion and fibroblast viability of human fibroblasts (Hs68) were measured in the presence of HADSCs-CM. The dermal layer, vascular endothelial growth factor (VEGF), and collagen levels were evaluated on the mice animal models between the treatments with and without HADSCs-CM.

Results: Western blotting, transmission electron microscopy (TEM), and dynamic light scattering (DLS) confirmed that the functional particles in HADSCs-CM were exosomes. When Hs68 fibroblasts were treated with HADSCs-CM, both cell viability and collagen secretion increased in a dose-dependent manner. Following the post-ultraviolet A (post-UVA) exposure, the mice exposed to the HADSCs-CM have decreased dermal thickness and VEGF expression and increased collagen volume compared to the non-HADSCs-CM exposed mice (control group).

Conclusion: HADSCs-CM significantly alleviated signs of skin senescence, including reduced dermal thickness, decreased VEGF expression, and enhanced collagen production. Exosomes, identified in the HADSCs-CM, are the functional component of these regenerative effects. This study highlights that the exosomal nanomedicine found in HADSCs-CM could regenerate skin, boost collagen production, improve fibroblast cell viability, and contain functional exosomes.

Keywords: adipocyte stem cells, collagen, dermal regeneration, exosomal nanomedicine, skin aging

Introduction

Skin is the largest organ of the human body, which has essential physical, chemical, and biological functions such as protecting organisms from external damage, maintaining fluid balance, and self-repair capabilities. Aging skin shows wrinkles, sagging, dullness, and roughness. Skin aging is a complex biological process influenced by both endogenous factors (eg, innate genes, hormonal changes, poor blood circulation) and exogenous factors (eg, sunshine exposure,

Received: 27 June 2024
Accepted: 5 November 2024
Published: 7 December 2024

Graphical Abstract

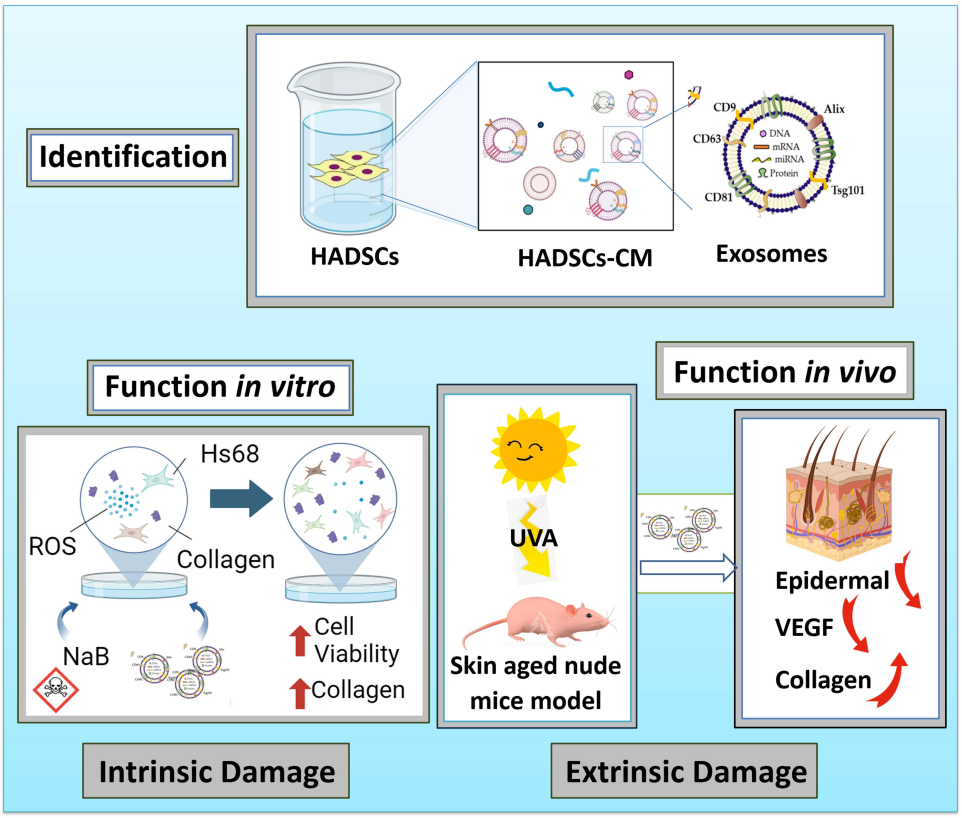

pollution, smoking, and dehydration).[1–3] A significant cosmetic complaint for senescent facial skin is the degradation and thinning of the subcutaneous and corium skin layers involved in the full appearance of the upper cheeks. The thinning of the skin between the zygoma and the mandible will be extremely visible as loose and sagging skin will lead to sunken cheeks.[4] With the gradual improvement of people's material living standards, there is increasing demand for effective anti-aging treatments that target to prevent and repair the skin from aging.

Several anti-aging strategies have been developed in the past few years, including lasers, dermal fillers, Botox, and hormone replacement therapy, but they are expensive and have safety concerns. Furthermore, Botox and fillers are temporary, and the re-treatment is recommended every 3–4 months due to the effects of botulinum toxin that relatively rapid the metabolism rate.[5] Consequently, there is a growing interest in finding safer and more effective alternatives. One natural and potential alternative for the skin aging issue is the procedure of adipose tissue transplantation that can improve the skin quality at the receptor site,[6] possibly due to the presence of mesenchymal stem cells in the adipose tissues. Stem cells are undifferentiated biological cells that differentiate into specialized cells that can produce more stem cells, which can be found within multiple organs and tissues.[7] Adipose-derived mesenchymal stem cells (ADMSCs) can be easily accessible and acquired through minimally invasive collection. These cells possess advantageous ideal properties including massive proliferation and easy adaptation when transplanted into a host, which made ADMSCs famous in anti-aging skin.[8]

Exosomes are small extracellular vesicles containing lipids, proteins, deoxyribonucleic acid (DNA), messenger ribonucleic acid (mRNA), and micro-ribonucleic acid (miRNA). These vesicles are then absorbed by peripheral cells, and their contents are deposited in the receiving cells. Exosomes play a critical role in intercellular communication between various types of cells. According to recent findings in cellular aging research, oxidative stress plays a significant

role in skin aging by accelerating up cellular damage, reducing the formation of collagen, and interfering with cellular communication.[9] Exosomes have the advantage of being tissue-specific, safe, and stable, along with the ability to cross the cellular bilayer to target specific cellular compartments, and can mitigate oxidative stress by enhancing cell viability and promoting the repair of damaged tissues, thus preventing and treating skin aging.[10] Additionally, exosomes are also called extracellular vehicles and nanovesicles, which have been demonstrated to be effective carriers in both artificial and cell-derived variants.[11]

Since ADMSCs were discovered, it is necessary to understand the repair effect and role mechanism of ADSMCs in association with various proteins, DNA, and RNA, especially the exosomes.[12] It is denoted that the repair effect involves vascular endothelial growth factor (VEGF) and transforming growth factor-β (TGF-β) secretions,[13] which can potentially be explicitly attributed to exosome proliferation and signaling. It is also known to promote intercellular communication between adjacent cells and distant cells. Providing supporting evidence connecting ADMSC-derived exosomes to cell-to-cell communication would be the first step in laying a foundation for preparing safe, effective, and inexpensive treatments for repairing senescent skin in the future. Hence, this study aims to evaluate the potential of ADMSC exosomes in reducing the effects of skin aging. The key parameters measured include fibroblast viability, collagen production, dermal thickness, and VEGF expression in mice models.

Materials and Methods

Chemicals and Reagents

Trypsin (Cat No.: 15050065), Roswell Park Memorial Institute (RPMI) 1640 Basal Medium (Cat No.: 11875093), stem cell osteogenic induction solutions (Cat No.: A1007201), collagenase type I (Cat No.: 17100017), and fetal bovine serum (Cat No.: 10099158) were purchased from Gibco. Human mesenchymal stem cell (MSC) analysis kit (Cat No.: 562245) was bought from BD Bioscience. UltraCULTURE Medium (Cat No.: 12–725F) was purchased from LONZA Corporation. Stem cell culture additive came from Fujian Yinfeng Bioengineering Technology Co., Ltd. Sodium butyrate (NaB, Cat No.: B5887) and 4',6-diamidino-2-phenylindole (DAPI, Cat No.: D9542) were bought from Sigma-Aldrich. Trypan blue staining solution (Cat No.: C0011), Masson staining kit (Cat No.: C0189S), Alcian blue (pH 2.5 color development kit, Cat No.: C0155S), cell counting kit (CCK)-8 (Cat No.: C0039), senescence-associated β-galactosidase (SA-β-gal) staining kit (Cat No.: C0602), and hematoxylin-eosin (H&E) dye (Cat No.: C0105S) were purchased from Beyotime Biotechnology Co., Ltd. 2',7'-dichlorodihydrofluorescein diacetate (H_2DCFDA, Cat No.: M07010) was purchased from Beijing Biolab Technology Co., Ltd. BODIPY^{TM} TR ceramide stain (Cat No.: D7540) was purchased from Thermo Fisher Scientific. While Anti-Cluster of Differentiation (CD) 81 (Cat No.: ab219209) and VEGF immunohistochemistry kits (Cat No.: ab1316) were purchased from Abcam.

Sample Preparation

Isolation of Human Adipose-Derived Stem Cells (HADSC)

Fat specimens (adipose tissues) collected from a liposuction surgery (patients have informed consent) were preserved in iceboxes at 4°C and delivered to the laboratory as soon as possible.[14] The adipose tissues were transferred into 50 mL centrifuge tubes at 40 mL for each tube, centrifuged at 800 g for 8 min. The tissues were then transferred to new centrifuge tubes that contained an equivalent volume of 0.9% normal saline for the washing process. The adipose tissues were centrifuged again at 800 g for 8 min. The supernatant was discarded, and the washing process was repeated three times.

The fat pellets were mixed with 0.075% type I collagenase on a shaker at 37°C with 120 rpm, to be digested for 45 min. The digested adipose tissues were then centrifuged at 800 g for 10 min. The upper layer of fat was discarded while the bottom pellets of stromal cells were suspended in specified media. The stromal cells were washed through procedures similar to those stated above. The washed cell pellets were re-suspended in RPMI 1640 media and filtered using a 100-mesh nylon mesh filter, followed by centrifugation of the purified cells at 800 g for 10 min. The cell pellets were re-suspended in 1 mL of RPMI 1640 media with 4 mL of pre-cooled erythrocyte lysate. The mixtures were left to stand for 4 min at room temperature to facilitate the erythrocyte lysis, centrifuged at 400 g for 5 min, and further re-

suspended in serum-free media. The purified cells were stained using trypan blue to adjust cell density at 7.0×10^5/mL. New media were pipetted into the cell suspension at a volume ratio 14:1 with further incubation in 37°C, 5% CO2, 95% humidity cell incubator (Forma™ Direct Heat CO2 Incubator 310, Thermo Fisher Scientific, USA). The cell media were replaced after 24 hrs to remove non-adherent cells, followed by the media refreshment every three days. After five days of culture, the cells were sub-cultured when the cell growth density reached approximately 90% confluency.

Co-Culture of HADSCs and Human Fibroblasts

Human fibroblasts (Hs68, BCRC Number: 60038, Bioresource Collection and Research Center) were cultured with the confluence HADSCs in Dulbecco's modified Eagle's medium (DMEM) supplemented 10% fetal bovine serum (FBS) and 1% antibiotic-antimycotic. The co-cultured cells were incubated at 37°C, 5% CO_2, and 95% humidity.[7]

Collection of HADSCs-CM

After the co-cultured cells reached 80% confluency, the serum-free media were discarded. The cells were washed twice with phosphate buffer saline (PBS), followed by the addition of serum-free RPMI 1640 media for starvation treatment. After 72 hrs of culture, the supernatants were collected and centrifuged at 300 g for 10 min to remove cell debris. Next, the centrifuged supernatants were filtered with 0.22 μm filter to obtain 100% HADSCs-conditional medium (HADSCs-CM). The preparation of 50% HADSCs-CM was done by adding 20 mL of RPMI 1640 media into 20 mL HADSCs-CM. The 25% HADSCs-CM was also prepared through a dilution process.

In-vitro Cell Analysis

Cell Viability Examination

Human fibroblasts (Hs68) were incubated with serum-free media (SFM) for 12 hrs to starve the cells. The media were aspirated after 24 hrs, adding 0%, 25%, 50%, and 100% HADSCs-CM to each well to replace the media every day for 5 consecutive days. The CCK-8 standard examination assessed cell viability by pipetting 10 μL of CCK-8 solution into each well before incubating in darkness for 1 hr at 37°C, 5% CO_2, and 95% humidity. An enzyme-linked immunosorbent assay (ELISA) analyzer reader was used to assess the absorbance at 450 nm. The control (0% HADSCs-CM), blank (SFM), and sample absorbance values (A) were used to calculate the cell viability percentage using Equation 1.

$$\text{Cell viability}(\%) = \frac{(A_{\text{sample}} - A_{\text{blank}})}{(A_{\text{control}} - A_{\text{blank}})} \times 100\% \quad (1)$$

Type I Collagen Secretion Examination

The concentration of collagen I released by the Hs68 in Section 2.3.1 was measured using the ELISA kit. Sequentially, biotinylated anti-human collagen 1α1 antibody, horseradish peroxidase-labeled avidin, and chromogenic substrate (3,3′,5,5′-Tetramethylbenzidine, TMB) were added into collagenase solution. A microplate reader was used to measure the optical density at the wavelength of 450 nm. A standard curve was used to calculate the concentration of collagen 1α1 at the detection range of 0.31–20 ng/mL.

In-vivo Animal Study

Animal Selection and Ethical Approval

Despite the in-vitro cell study, the cell-to-cell communication was investigated physiologically through *in-vivo* animal study in 24 male healthy nude mice (BALB/c-Foxn1nu/Nju), 8-week-old, specific-pathogen-free (SPF) grade, 20 ± 2 grams. The mice were acclimatized for 1 week prior to the experiment under controlled temperature (22±2°C) and a 12-hour light/dark cycle. All manipulations were done to minimize animal suffering with a proper animal handling, approved by the animal committee.[7]

Preparation of Concentrated HADSCs-CM

Prior to the *in-vivo* animal study, the concentrated HADSCs-CM was prepared by centrifuging the HADSCs-CM at 300 g for 10 min. The supernatant was collected and filtered with 0.22 μm filter. Next, the supernatant was further centrifuged at 3,500 g at 4°C with the adoption of 10 kDa molecular weight ultrafiltration tube to separate the secretory group to

obtain 40× HADSCs-CM concentration. The concentrated HADSCs-CM was stored at −20°C. The 40× concentration was also diluted into 20× and 10× concentrations.

Preparation of Concentrated Sodium Butyrate (NaB) Solution

The concentrated NaB solution was prepared by adding 0.527 g NaB powder into 300 mL sterile distilled water to obtain 16 mM concentration. Next, the 16 mM concentration were also diluted into 1, 2, 4 and 8 mM concentrations, respectively.[15]

Aging Skin on Nude Rat Model

Nine healthy male nude mice were divided into 3 groups with each group being kept in a separate cage. The nude mice in group A were used as blank control. The ultraviolet A (UVA) at the wavelength of 350 nm (threshold value = 10 mJ/cm^2) was irradiated to the mice in groups B and C for 90 min, every two days. The Group B mice was irradiated for 3 days with a cumulative irradiation of 20 mJ/ cm^2, while the Group C mice was irradiated for 9 days with a cumulative irradiation of 50 mJ/ cm^2. On the 10th day, all mice were sacrificed by the cervical dislocation method, followed by the peeling of nude mouse's back skin for further analyses to identify which UVA threshold limit value are most suitable to be irradiated as the aged nude mice development examination conditions.[16]

HADSCs-CM Repair Ability Examination

The 15 nude mice were divided into 5 groups. The first group was the blank control. The 2nd group was the negative control group, and the 3rd to 5th groups were the experimental groups to testify the repaired ability on different HADSCs-CM concentrations. The 2nd to 5th mice groups were irradiated with UVA at the wavelength of 350 nm (10 mJ/cm^2) for 90 min, every second day for five times. On the 10th day, 0.15 mL of the 10×, 20×, and 40× concentrated solutions of HADSCs-CM were injected subcutaneously in Group 3–5, respectively. The HADSCs-CM was injected again on the 20th day. On the 30th day, 5 groups of nude mice were sacrificed by the cervical dislocation method with the back skins immediately removed and fixed in formalin.[5]

Hematoxylin and Eosin Tissue Staining

The collected tissues were dried and re-hydrated in a fume hood. The tissues were then immersed in hematoxylin for 3 min, followed by the rinsing procedure with distilled water until the tissues turned blue. Tissue dissociation was done using 1% hydrochloric acid alcohol for several seconds. Next, the dissociated tissue samples were soaked in 1% ammonia solution for several seconds, and then the immersion in eosin was done for 3 min. Finally, the samples were dehydrated for 5 min using 95% ethanol and anhydrous ethanol in sequence, preserved in the glue, dried naturally, and stored in a 4°C refrigerator to be visualized under a microscope at (Nexcope NIB-600, Ningbo Yongxin Optics Co., Ltd., China).[5]

Masson Tissue Staining

First, the formalin-fixed dewax samples from Section "HADSCs-CM repair ability examination" were set into 100 µL of Masson composite-staining solution for 5 min. The dye solution was rinsed with distilled water. An amount of 100 µL of phosphomolybdic acid and aniline blue were then added dropwise for 5 min, in sequence individually. The samples were rinsed with distilled water and dissociated using 100 µL of differentiation solution in Alcian blue color development kit, twice for 30–60 seconds. Finally, the dissociated samples were dehydrated with 95% alcohol and anhydrous alcohol to be visualized under the microscope. In the staining results, the aniline blue stained the collagen fibers, mucus, cartilage, and nerve fibers in blue color.

VEGF Expression Examination

The immunohistochemical method was used to measure VEGF expression. The samples were immersed wholly in 300 mL of citrate buffer, rinsed three times, 3 min each, with Tris-buffered saline (TBS). The antigen retrieval was used in an antigen retrieval pot at 110°C for 5 min under high pressure. The hydrogen peroxide solution was added to block the activity of endogenous peroxidase. The non-antigen-binding sites were blocked on each tissue, followed by the incubation of the primary antibody. Next, 30 µL of rabbit anti-VEGF antibody (rabbit anti-VEGF antibody and 5% BSA diluted at a ratio of 1:50) was adopted to each tissue with the sequential addition of the secondary antibody for 3 min.

After drying the slides, streptavidin-peroxidase was pipetted for 10 min, and the tissues were washed with TBS. The samples were dried again, followed by adding 3.3′-diaminobenzidine (DAB) color development solution to develop the DAB. The hematoxylin was used to stain the samples where the stained samples were dehydrated with a series of ethanol concentrations, 70–95%, and absolute ethanol in sequence for 3–5 min, individually. Finally, the 70% neutral gum was covered on the samples, dried naturally in the air, and visualized under a microscope.

Exosome Identification

Isolation of Exosome

The HADSC's secretomes from −80°C were thawed at 4°C overnight in the fridge and centrifuged for 10 min at 300 g and 4°C. The supernatants were centrifuged at three different parameters: 2,000 g for 15 min, 10,000 g for 30 min, and 100,000 g for 90 min, separately to preserve the supernatants. Finally, 200 µL of PBS was added to the supernatants and centrifuged at 100,000 g for 90 min to preserve the precipitates.

Bicinchoninic Acid Assay

To develop a standard curve, the 1.0, 0.5, 0.25, 0.125, 0.0625, and 0 mg/mL of exosomes were diluted using the standard bovine serum albumin (BSA). In a 96-well plate, the 25 µL samples were treated with the standard BSA solution and 200 µL color-developing solution. The 96-well plate was incubated at 37°C for 40 min, protected from light. Next, the optical density was measured at 562 nm using a microplate reader, followed by calculating protein concentration by referring to the standard curve.

Particle Characterization

Transmission electron microscopic (TEM) images were obtained using a transmission electron microscope (H-7000 FA, HITACHI, Japan) to view the morphology of the exosomes. The images were further analyzed using the image analysis software (Image J, NIH, USA). Dynamic Light Scattering (DLS) was used to analyze and measure the particle size distribution of exosomes by using dynamic light scattering instrument (nanoSAQLA, Otsuka Electronic, Korea).

Western Blot Assay

Cells were cultured in a 10-cm dish, once the cellular volume reached 70%, it is ready for proteins extraction. Next, the protein was quantified by using the bicinchoninic acid (BCA) protein assay. The protein on a 10% gel was separated by SDS-PAGE, then transferred to the polyvinylidene fluoride (PVDF) membrane (Bio-Rad Laboratories, Hercules, CA, USA). The membranes were covered by 5% skim milk, and incubated for another day at 4°C with the specific primary antibodies (COX2, p38, and GAPDH). The secondary antibody was then added, and the mixture was incubated for one more hour. The Mini Chemi^{TM} Chemiluminescence Imaging System was then used to examine the PVDF membrane in order to see the stained blots and identify the protein bands.[16]

In vitro Tracking Experiments of Exosomes

This study used the BODIPY^{TM} TR Ceramide reagent to stain the exosome membrane in red. Initially, the exosome solution was mixed with 1 mL of RPMI 1640 basal medium. Then, 1 µL of BODIPY^{TM} TR Ceramide stain was added, followed by 25 mL RPMI 1640 basal medium at a later 30 min. The mixed solution was centrifuged at 100,000 g at 4°C for 90 min. The supernatant was discarded, and the washing process was continuously conducted using PBS to remove the remaining dye. The washed solution was centrifuged at similar parameters to obtain the stained exosomes. The stained exosomes were then isolated and co-cultured with the Hs68 in a serum-free medium. After washing the cells, the exosomes that had entered the cells were left in the cell culture dish and treated with 4% Polyoxymethylene. The cells were fixed with formaldehyde and DAPI to be observed under a confocal fluorescence microscope.[11]

Co-Culture of Exosomes and Hs68

The Hs68 were co-cultured with fresh RPMI 1640 basal medium for 18 hrs at normal incubation parameters (37°C, 5% CO2, 95% humidity). DAPI staining solution was then added to stain the nuclei for 5 min. The staining solution was

washed away, followed by the observation, and photographed using a laser confocal fluorescence microscope (Nexcope NIB900, Ningbo Yongxin Optics Co., Ltd., China).

Statistical Analysis

The homogeneity of variance test and normality test were carried out to determine the level of output accuracy. The comparison between the means of multiple data groups was performed by one-way analysis of variance at $p<0.05$ where the non-parametric test was used for those with unequal variance. All statistical analyses in this study were performed using SPSS 11.5 statistical processing software (Version 11.5, International Business Machines Corporation (IBM), USA).

Results

Hs68 Cell Viability and Reactive Oxygen Species (ROS) Presence

To find a proper amount of NaB demonstrating the anti-aging function of HADSCs-CM, different NaB concentrations were incubated with Hs68 for 48 hrs. The cell viability of Hs68 was examined by the CCK-8 kit (Figure 1A). The proliferative of Hs68 in 2 mM NaB is acceptable at the viability of 75%. Obviously, at 16 mM NaB, the cell death was over 50%. Thus, 4 and 8 mM NaB are established as the senescent trigger standard.

The accumulation of ROS is the marker for cell damage, stress, and age. The H_2DCFDA has been used as the probe because the ROS could oxidate the H_2DCFDA into dichlorofluorescein (DCF), to be detected by a flow cytometry. After

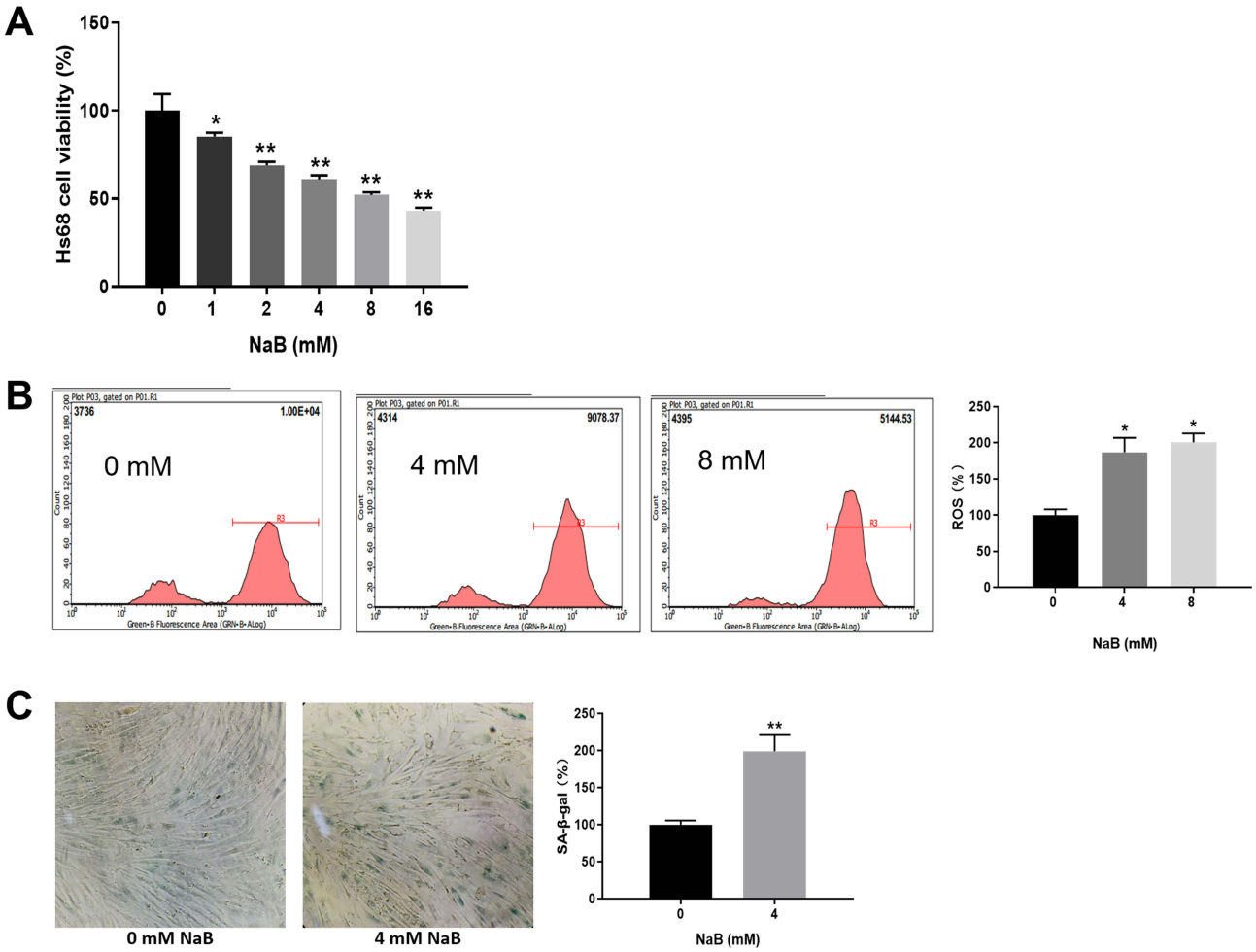

Figure 1 (**A**) Hs68 cell viability in different NaB concentration after 48 hrs from 0 to 16 mM. (**B**) Intracellular ROS of Hs68 in different NaB dosage treatments. (**C**) SA-β-gal stained Hs68 after 0 and 4 mM NaB treatments. n=3, *p<0.05, and **p<0.01.

incubating the Hs68 in 0, 4, and 8 mM NaB for 48 hrs, the intracellular ROS levels significantly increased when the dosage of NaB was induced. The free radicals in Hs68 were double in 4 and 8 mM NaB compared to the control group (Figure 1B). However, there was no significant difference in ROS levels between the 4 and 8 mM NaB treatments. Therefore, the 4 mM NaB treatment would induce the senescence of Hs68 fibroblasts.

The SA-β-gal is also a decent biomarker for cell aging. Thus, the SA-β-gal staining method was applied to testify to the SA-β-galactosidase activity. The photomicrographs show the area of SA-β-gal stained Hs68 after the treatments with 0 and 4 mM NaB at 48 hrs. The SA-β-gal stained images were analyzed by Image J software. The results show that the SA-β-galactosidase activity in 4 mM NaB was significantly higher than the 0 mM NaB treatment (Figure 1C). Consequently, the senescence ability in NaB is substantiated, where the 4 mM NaB was selected as the proper amount of aging provoker in the coming experiment.

Hs68 in the Presence of HADSCs-CM

The Hs68 cells were incubated in the medium of various HADSCs-CM concentrations for 1 to 5 days where the CCK-8 kit was used to testify to the cell viability. The results revealed that the cell viability was proportional to the concentration of HADSCs-CM and the period, especially after 3 days of incubation. The cell survival rates were significantly boosted to 150% when the Hs68 cells were incubated at 5 days with 25% HADSCs-CM, and 4 days with 50% and 100% HADSCs-CM. On the 5th day, the incubation with 50% and 100% HADSCs-CM cause the Hs68 cell viability to reach almost twice compared to the control group. During 3 days of adopting 25% HADSCs-CM, the proliferative viability was 50% more than the control group (Figure 2). The results showed that the HADSCs-CM has successfully improved the cell viability of Hs68 fibroblasts.

HADSCs-CM Treatment in Conjunction with NaB Exposure

The experiments were divided into two groups. One group of the experiments involved incubating different concentrations of HADSCs-CM for 48 hrs first. Then, the 4 mM NaB was used as an aging agent to induce the cell senescent procedure (Figure 3A and B). The other group of experiments involved the reverse flow, with the NaB procedure as the first part, followed by the treatment with different concentrations of HADSCs-CM (Figure 3C and D). The cell viability and the emission rate of collagen 1α1 were recorded in both groups of the experiments.

In post-treated 4 mM NaB, the cell viability significantly declined. The cell viability in the pre-treatment of HADSCs-CM at ×2.5, ×5, ×10, and ×20 concentrations was approximately 1.5 times higher than the negative group. However, all results in the experimental groups were significantly lower than the control group. It might show that the pre-treatment of HADSCs-

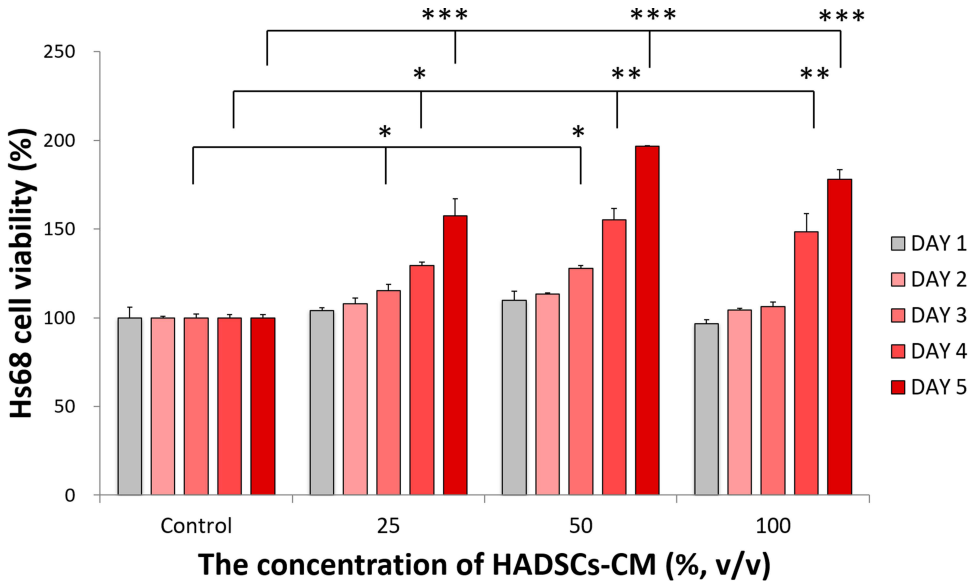

Figure 2 Examination of different concentrations of HADSCs-CM on Hs68 cell viability. n=3, *p<0.05, **p<0.01, and ***p<0.005.

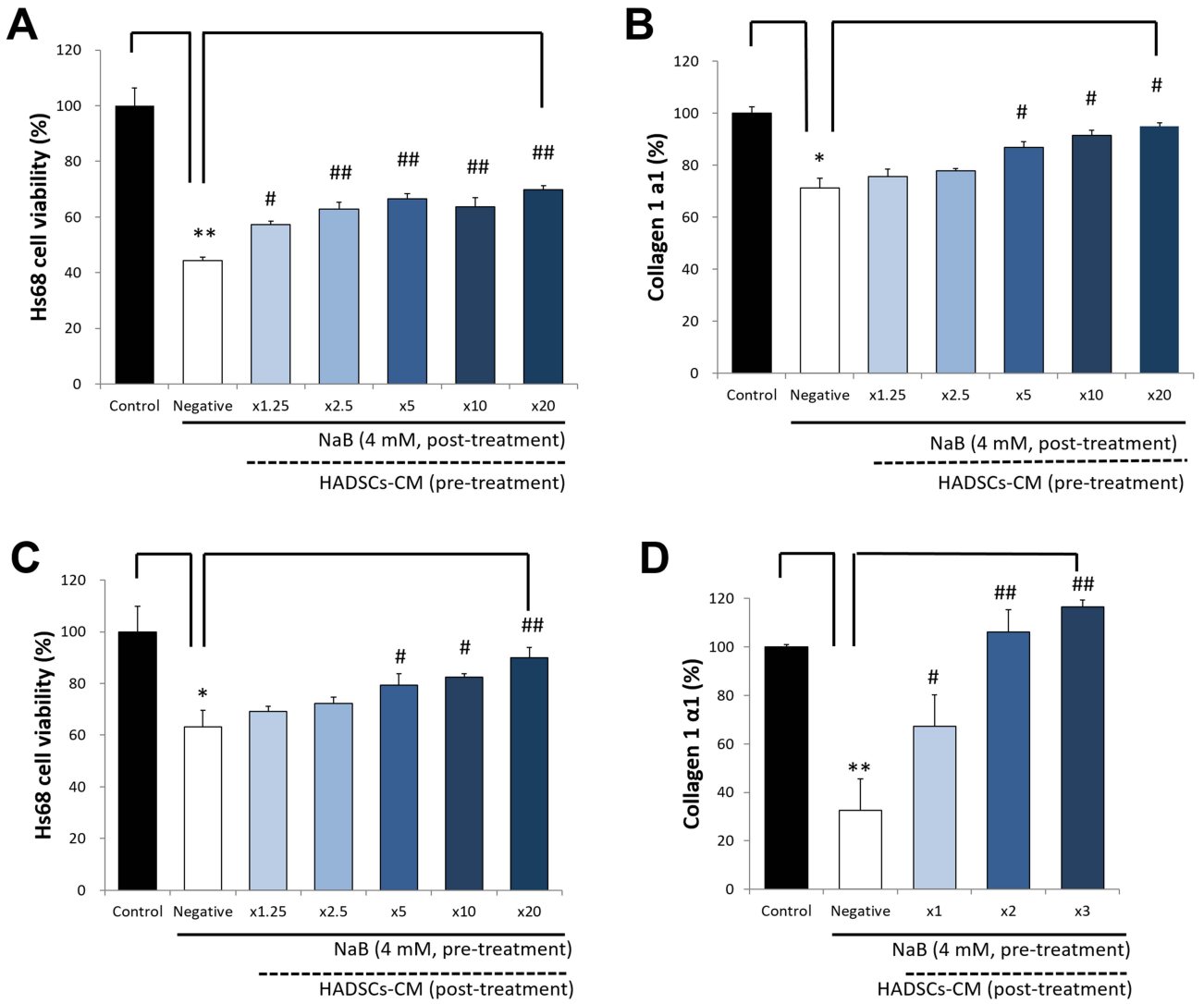

Figure 3 Effects of HADSCs-CM in preventing Hs68 fibroblast senescence. (**A**) Pre-treatment effect of HADSCs-CM in decreasing Hs68 fibroblasts cell viability. (**B**) Consequences of HADSCs-CM pre-treatment in increasing collagen release from Hs68 fibroblasts. (**C**) Post-treatment effect of HADSCs-CM in lowering Hs68 fibroblasts cell viability. (**D**) Consequences of HADSCs-CM post-treatment in increasing collagen release from Hs68 fibroblasts. n=3, *p<0.05 and **p<0.01 comparison to control group; and #p<0.05, ##p<0.01 comparison to negative group.

CM could not entirely prevent the damage from NaB. However, the post-treatment results for different concentrations of HADSCs-CM demonstrated that the cell viability in HADSCs-CM treatments was significantly higher than in the negative group. Notably, the cell survival rate in the ×20 hADSCs-CM group was close to the control groups. It might represent the effectiveness of HADSCs-CM on the reparation damage rather than preventing the injury in Hs68. On the other hand, in the ×5, ×10, and ×20 hADSCs-CM pre-treated groups, the collagen secretion rate was significantly higher than the negative group but slightly lower than the control group. The post-treatment of HADSCs-CM experiments revealed great results in the presence of HADSCs-CM. The collagen excretion rates in ×2 and ×3 hADSCs-CM were almost near or slightly higher than the control group. The results convince us that the HADSCs-CM had a distinct ability to recover collagen emission. Compared to the negative group in the pre-treatment of HADSCs-CM and the post-treatment of HADSCs-CM, the collagen-produced rates in the pre-treated HADSCs-CM were lower than in the post-treatment of HADSCs-CM. The HADSCs-CM has prevented the loss of collagen quantity marginally. However, the results in the post-treatment of HADSCs-CM were more significant. Thus, the post-treatment of HADSCs-CM was exploited in the following *in-vivo* experiments.

The Aged Skin Nude Mice Model

The NaB induction was not appropriate for the skin of nude mice because the nude mice would take the NaB as food, thus declining the function of aging. Therefore, different dosages of UVA irradiation were applied instead. The dermal thickness increased by dose-dependent as seen in the microscopy images and H&E staining. The 50 J/cm^2 UVA irradiated dermal skin was significantly thicker, 26.5%, than the control group (Figure 4A). The Masson staining results illustrated that the collagen volume in the irradiated 50 J/cm^2 UVA was looser by 17% than the control group (Figure 4B). The dermal thickness and collagen volume have no significant difference between the control and 20 J/cm^2 UVA irradiated groups. Therefore, the 50 J/cm^2 UVA would be irradiated as the aged nude mice development examination conditions.

The presence of HADSCs-CM recovered the aged and thicker skin, showing dose-related function. The higher concentration of HADSCs-CM presented thinner dermal skin in the nude mice. All three groups of HADSCs-CM revealed significant results. The HADSCs-CM repaired the aged skin at 12%, 15%, and 17% lower than the negative control (Figure 4C). The

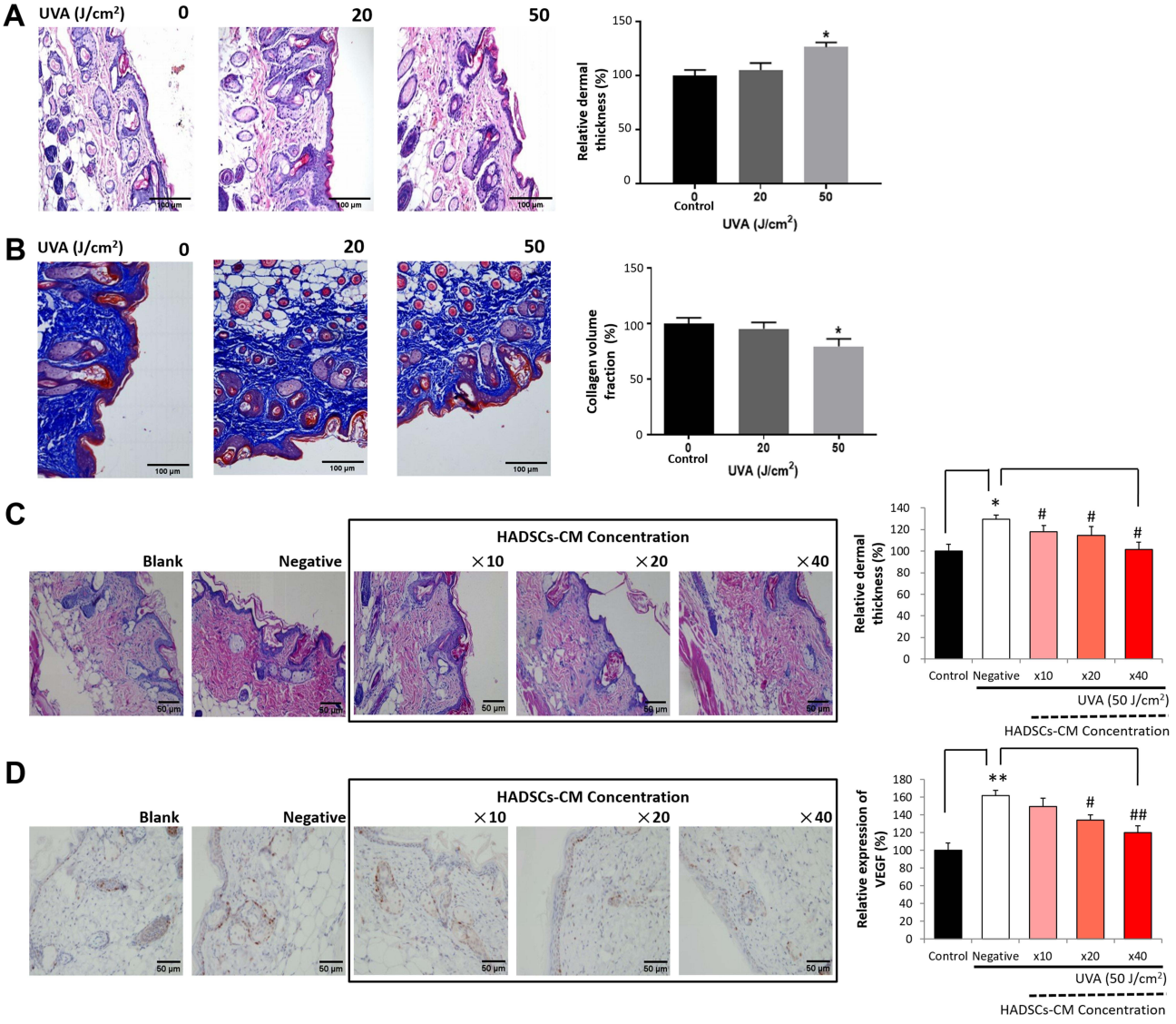

Figure 4 Aged skin model from nude mice. (**A**) Dermal thickness after 0 (control group), 20, and 50 J/cm^2 UVA irradiation (×200). Thickness-increasing percentage was measured by SmileView. (**B**) Dermal collagen expression after UVA irradiation. An increasing percentage of collagen emission was measured by Image J. (**C**). Different concentrations of HADMSC-CM affected dermal thickness after 50 J/cm^2 UVA irradiation. Dermal thickness measured by SmileView. (**D**) ×10, ×20, and ×40 concentrated HADSCs-CM affected VEGF secretion, increasing on senescent skin nude mice. Expression of VEGF was measured by Image J. n=3, *p<0.05 or **p<0.01 compared with the control group; #p<0.05, ##p<0.01 compared with the negative group.

HADSCs-CM has a specific function in repairing aged skin. To ensure the HADSCs-CM could adjust the thickness of the ancient dermal layer of the nude mice, VEGF was examined by immunohistochemistry, followed by the image evaluation using Image J. The ×20 and ×40 hADSCs-CM concentrations also significantly reduced the VEGF quantity, 27.4% and 41.7% lower than the negative control in the ×20 and ×40 hADSCs-CM concentrations (Figure 4D). The effects of HADSCs-CM might affect the aged dermal skin by adjusting the VEGF expression rate.

Functional Particle Identification

The TEM, DLS, and Western blot revealed the presence of exosomes in the HADSCs-CM. The results show spherical microbubbles with cup-shaped structures by TEM. The particle size of the microbubbles was measured by DLS, which was around 50–200 nm, and the CD81 cell markers were distinguished by Western blot (Figure 5A). The exosomes were ensured in the HADSCs-CM after the three methods below. Ultra-high-speed centrifugation was used to isolate the exosomes of the HADSCs-CM. The density of human adipose-derived stem cells conditional medium-exosomes (HADSCs-Exos) was 0.424 mg/mL, evaluated by the BCA protein quantitative kit. The Hs68 cell viability would represent the effects of HADSCs-Exos and therefore, has been examined by the CCK-8 assay in this study. 0, 25, 50 μg/mL HADSCs-Exos was conducted in the RPMI 1640 medium and incubated with the Hs68 cells for 1 to 5 days. The 50 μg/mL HDSCs-CM increased the cell viability within 2 to 5 days, with the records of 175%, 202%, 307%, and 389%, respectively. The 25 μg/mL HDSCs-CM also significantly improved the cell viability after 3 days of incubation (Figure 5B). The results show that the exosomes affected the Hs68 cell viability, offering the dose- and time-dependent effects.

The interaction between exosomes and the Hs68 cells was observed using BODIPY^{TM} TR Ceramide and DAPI staining methods. The BODIPY^{TM} TR Ceramide was used as a stain for phospholipids. The DAPI was a blue-fluorescent

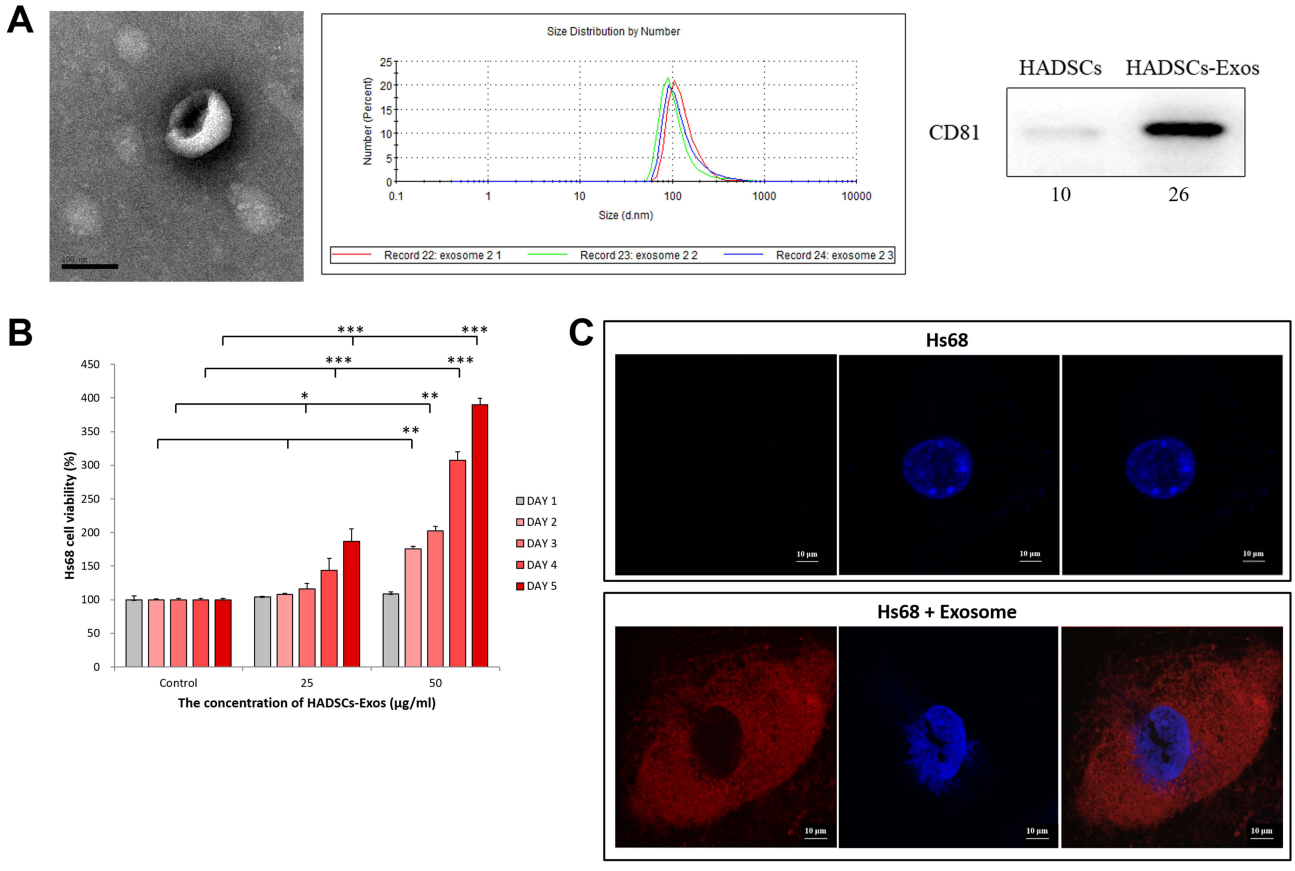

Figure 5 Identification of exosomes. (**A**) TEM took the exosome microphotograph at x400k magnification. Dynamic Light Scattering measures the exosome's size distribution. Cell marker CD81 was detected on exosomes by Western blotting. (**B**) Cell viability was affected by a variety of concentrations of HADSCs-Exos. (**C**) BODIPY^{TM} TR Ceramide and DAPI distinguished the phospholipid layers of exosomes and the cell nucleus of Hs68. Merged photo shows exosomes and Hs68 cell interactions. n=3, *p<0.05, **p<0.01, and ***p<0.005.

DNA stain that enhanced fluorescence upon binding to AT regions of dsDNA. The BODIPY^{TM} TR Ceramide stained the phospholipid of exosomes in red fluorescence, and the DNA of Hs68 was stained by DAPI in blue color, separately, distinguished the phospholipid layers of exosomes and the cell nucleus of Hs68. After 18 hrs of staining, the exosomes and the Hs68 were cultured and observed through fluorescence. The margin photo shows that with and without the exosomes entered the Hs68 fibroblasts (Figure 5C).

Discussion

Aging is the spontaneous and inevitable process of organisms over time. It is a complex, natural phenomenon manifested by structural and functional decline, weakened adaptability, and decreased resistance of the skin layer. It is also affected by endogenous (genetic, cellular metabolism, hormone, metabolic processes, etc.) and exogenous (chronic light, contamination, ionizing radiation, chemicals, toxins, etc.) factors.[2,17,18] The luster and elasticity of skin largely depend on collagen and elastin synthesized by fibroblasts in the dermis layer of the skin. Several studies explained that DNA damage, waste metabolite accumulation, increased free radicals, and cross-linking macromolecules with glycosylation could speed up the senescent process.

The NaB and UVA were separately conducted in this research to establish an aging model in Hs68 fibroblasts and nude mice skin. Previous studies have shown that NaB can induce cellular senescence in various cell types.[19] Signs of senescence include increased cytoplasmic size, nuclear dispersion, and elevated reactive oxygen species (ROS) levels.[20–22] The free-radical level could be detected by a flow cytometry, while the SA-β-gal staining could reveal the SA-β-galactosidase activity.[23] From the results of this study, it has been confirmed that the NaB could enhance the ROS and SA-β-galactosidase activity levels within the Hs68, and the aging process was NaB dose-dependent. The quantity of collagen secreted by Hs68 cells significantly decreased after NaB treatment, with 4 mM NaB being identified as the optimal dose for establishing the Hs68 senescence model.

Solar radiation was used to simulate an extrinsic factor of aging.[2] Solar UV radiation could be divided into UVA, ultraviolet B (UVB), and ultraviolet C (UVC). Ambient sunlight is mainly UVA (90% ~95%) and UVB (5%–10%), while the ozonosphere absorbs UVC.[24] The UVA, with a wavelength between 315 and 400 nm, can penetrate deeply into the dermis, generating ROS efficiently and further causing damage to DNA and other macromolecules. When the UV dose is overabundant, keratinocytes will initially activate the apoptosis progress.[2,25] However, after several hours of UV exposure, the damage signals change, reforming the cell cycle suppressed by keratinocytes through various epidermal growth factors, leading to increased epidermal thickness through VEGF abundance.[26] Furthermore, free radicals generated by UVA will result in skin aging and declining collagen emission. The aged skin mice model confirmed that the aged skin had thicker dermal, less collagen generation, and more VEGF.

Many studies showed that the HADSCs-CM could enhance skin collagen production, angiogenesis, and cell proliferation, inhibit apoptosis, promote skin barrier function repair, and reduce inflammation in skin lesions.[13,27] In the experiment, it is testified that the HADSCs-CM has potent abilities to improve the cell viability in Hs68 by repairing the damage from chemicals (Figure 3), increasing the emission of collagen, decreasing the thickness of the dermal layer in aged skin, further eliminating the VEGF quantity in the skin. Despite the HADSCs-CM performing better post-treatment than in pre-treatment when the NaB was adopted into the Hs68 cells, the HADSCs-CM can compensate for the chemical damage to the skin to a certain extent. Some studies also approved that the functional material in HADSCs-CM is exosomes, which could provide bio-functionality.[27,28]

Exosomes have been recognized as intercellular communicators between many cell lines. Several studies reported that DNA, RNA, small-interfering ribonucleic acid (siRNA), proteins, and other chemicals could be transmitted by exosomes and released by normal cells or cancer cells.[10,14] Exosomes in cancer cells can participate in various physiological and pathological processes, such as tumor development, growth, progression, metastasis, and drug resistance development.[14] Exosomes are virus-like particles. The grain size is between 50 and 200 nm, and there are CD9, CD63, and CD81 markers on the outer membrane.[29] In the experiments, it has been proven that exosomes could positively affect fibroblast cells, which can expand the Hs68 lifespan, double the collagen released quantity, and revive the damage from the ROS.

The density gradient ultracentrifugation (DGUC) has been used to purify the exosomes in the HADSCs-CM. The TEM, DLS, and Western blotting have been used to substantiate the existence of exosomes in the HADSCs-CM. The purified

exosomes show a significant ability to improve the Hs68 cell viability. Exosomes could fuse into the cytosol of target cells. The lipid, integrins, and adhesion chemicals on the surface exosomes also mediate the interaction and attachment between exosomes and the target cells.[11] The lipophilic dye BODIPY^{TM} TR could help distinguish endocytosis from fusion, and the nucleic acid stain DAPI could notify the contained DNA transfer from exosomes into cells. The endocytosis of exosome entry occurs in most cell types, for instance, ovarian and colon tumor cells, cardiomyocytes, macrophages, hepatocytes or neural cells, and epithelial cells.[30] The results illustrate the red fluorescent phospholipid, which BODIPY^{TM} TR dyes have been characterized surrounding the Hs68, and the blue, fluorescent nucleotide was inside the cell. The fibroblasts may also have the same fusion mechanism as most cells.

This study confirms the effects of HADSCs-CM on preventing skin aging and functional elements being exosomes. First, HADSCs-CM could increase the collagen emission rate and the cell viability in vitro after NaB conducting. Moreover, in vivo, the HADSCs-CM could reduce the symptoms of senescence in the skin, which has seduced aging, including thinner epidermal, less VEGF, and more collagen than the control group. Then, ultracentrifugation was used to analyze the functional components in HADSCs-CM. The element could be found in the sediment of HADSCs-CM. After cell markers confirmation, TEM observation, and DLS analysis, the characteristics of features are the same as exosomes. Thus, cell viability has been conducted to verify that the valuable component in HADSCs-CM is exosome.

This study shows that exosomes derived from HADSCs can reduce dermal thickness, increase VEGF expression, and improve collagen production; however, it is limited by not investigating long-term effects and other mechanisms, such as the involvement of important signaling pathways. In order to improve the therapeutic applications of exosomes in skin aging, future research should concentrate on studying these pathways, carrying out clinical trials to assess the long-term efficacy and safety of exosome-based treatments, and investigating broader functional outcomes like fibroblast proliferation and extracellular matrix (ECM) expression.

Conclusion

In conclusion, this study investigates the aging process in Hs68 fibroblasts and nude mice skin induced by NaB and UVA radiation. NaB is found to accelerate the senescence process in Hs68 cells in a dose-dependent manner, leading to increased ROS levels, SA-β-galactosidase activity, and a reduction in collagen emission. UVA radiation simulates an extrinsic factor of aging, causing skin damage, increased epidermal thickness, reduced collagen generation and VEGF expression. The study demonstrates that HADSCs-CM, particularly its exosome components, can mitigate the effects of aging. HADSCs-CM enhances cell viability, and collagen production, and reduces skin senescence symptoms in vivo models. The findings support the potential therapeutic role of exosomes in preventing skin aging and highlight their functional significance in promoting skin health.

Highlights

- Physical/chemical damage factors in skin health.
- ADSC conditional medium reverses damages.
- Exosomes confirmed to be functional nanoparticles.

Abbreviations

HADSCs-CM, Human adipose-derived stem cells conditional medium; Hs68, human fibroblasts; VEGF, vascular endothelial growth factor; TEM, Transmission electron microscopic; DLS, Dynamic Light Scattering; UVA, ultraviolet A; ADMSC, Adipose-derived mesenchymal stem cell; DNA, deoxyribonucleic acid; mRNA, messenger ribonucleic acid; miRNA, micro-ribonucleic acid; TGF-β, transforming growth factor-β; RPMI, Roswell Park Memorial Institute; MSC, mesenchymal stem cell; DAPI, 4',6-diamidino-2-phenylindole; CCK, cell counting kit; SA-β-gal, senescence-associated β-galactosidase; H2DCFDA, 2',7'-dichlorodihydrofluorescein diacetate; CD, cluster of differentiation; DMEM, Dulbecco's modified Eagle's medium; FBS, fetal bovine serum; SFM, serum-free media; ELISA, enzyme-linked immunosorbent assay; TMB, 3.3′,5.5′-Tetramethylbenzidine; SPF, specific-pathogen-free; NaB, Sodium Butyrate; TBS, Tris-buffered saline; DAB, 3.3′-diaminobenzidine; BSA, bovine serum albumin; PVDF, polyvinylidene fluoride; ROS, reactive oxygen species; DCF, dichlorofluorescein; HADSCs-Exos, human adipose-derived stem cells conditional

medium-exosomes; UVB, ultraviolet B; UVC, ultraviolet C; siRNA, small interfering ribonucleic acid; DGUC, density gradient ultracentrifugation; ECM, extracellular matrix.

Data Sharing Statement

The authors confirm that all data is fully available without restriction. All relevant data are described within the paper.

Animal Ethics Statement

The animal ethical approval for conducting an *in-vivo* animal study was obtained from Huaqiao University's Institutional Animal Care and Use Committee with the approval license number A2016043. The experimental procedure followed the guidelines outlined by the Animal Care Services at Huaqiao University.

Human Ethics Statement

The human ethical approval for collecting fat specimens (adipose tissues) from liposuction surgery was obtained from Huaqiao University's School of Medicine with the approval license number M2016015. The patients gave informed consent, and the experimental procedure followed the guidelines outlined in the Declaration of Helsinki.

Acknowledgments

This research was supported by the Ministry of Science and Technology (MOST), Taiwan, under grant nos. MOST 111-2221-E-005-009. MOST 110-2221-E-039-002-MY3. We also acknowledge and appreciate the assistance from Dr Ming-Shan Chen, Dr Wei-Chih Lien, Gizem Naz Canko, and Tzu-Yu Lin in the experiment and manuscript preparation.

Disclosure

The author(s) report no conflicts of interest in this work.

References

1. Li J, Lu Y, Lin I, et al. Reversing UVB-induced photoaging with hibiscus sabdariffa calyx aqueous extract. *J Sci Food Agri*. 2019;100(2):672–681. doi:10.1002/jsfa.10063
2. Krutmann J, Schikowski T, Morita A, Berneburg M. Environmentally-induced (extrinsic) skin aging: exposomal factors and underlying mechanisms. *J Invest Dermatol*. 2021;141(4):1096–1103. doi:10.1016/j.jid.2020.12.011
3. Ganesan P, Choi DK. Current application of phytocompound-based nanocosmeceuticals for beauty and skin therapy. *Int J Nanomed*. 2016;1987–2007. doi:10.2147/IJN.S104701
4. Gao J, Wang X, Qin Z, et al. Profiles of facial soft tissue changes during and after orthodontic treatment in female adults. *BMC Oral Health*. 2022;22(1):257. doi:10.1186/s12903-022-02280-5
5. Wee SY, Park ES. Immunogenicity of botulinum toxin. *Arch Plastic Surg*. 2022;49(01):12–18. doi:10.5999/aps.2021.00766
6. Dong J, Wu B, Tian W. Preparation of apoptotic extracellular vesicles from adipose tissue and their efficacy in promoting high-quality skin wound healing. *Int J Nanomed*. 2023;18:2923–2938. doi:10.2147/IJN.S411819
7. Wang HM, Chou YT, Wen ZH, Wang CZ, Chen CH, Ho ML. Novel biodegradable porous scaffold applied to skin regeneration. *PLoS One*. 2013;8(11):e56330.
8. Yang X, Meng H, Peng J, et al. Construction of microunits by adipose-derived mesenchymal stem cells laden with porous microcryogels for repairing an acute achilles tendon rupture in a rat model. *Int J Nanomed*. 2020;15:7155–7171. doi:10.2147/IJN.S238399
9. Bellei B. Focus on the contribution of oxidative stress in skin aging. *Antioxidants*. 2022;11(6):1121. doi:10.3390/antiox11061121
10. Cheng YC, Chang YA, Chen YJ, et al. The roles of extracellular vesicles in malignant melanoma. *Cells*. 2021;10(10):2740. doi:10.3390/cells10102740
11. Chen C, Wang J, Sun M, Li J, Wang HMD. Toward the next-generation phyto-nanomedicines: cell-derived nanovesicles (CDNs) for natural product delivery. *Biomed Pharmacother*. 2022;145:112416.
12. Jang SC, Crescitelli R, Cvjetkovic A, et al. Mitochondrial protein enriched extracellular vesicles discovered in human melanoma tissues can be detected in patient plasma. *J Extracell Vesicles*. 2019;8(1). doi:10.1080/20013078.2019.1635420
13. Cheng YS, Yen HH, Chang CY, et al. Adipose-derived stem cell-incubated ha-rich sponge matrix implant modulates oxidative stress to enhance VEGF and TGF-β secretions for extracellular matrix reconstruction *in vivo*. *Oxid Med Cell Longev*. 2022;2022:1–17.
14. Nail HM, Chiu CC, Leung CH, Ahmed MM, Wang HMD. Exosomal MIRNA-mediated intercellular communications and immunomodulatory effects in tumor microenvironments. *J Biomed Sci*. 2023;30(1). doi:10.1186/s12929-023-00964-w
15. Liu X, Jiang C, Liu G, et al. Sodium butyrate protects against oxidative stress in human nucleus pulposus cells via elevating PPARγ-regulated Klotho expression. *Int Immunopharmacol*. 2020;85:106657. doi:10.1016/j.intimp.2020.106657
16. Lin ET, Lee YC, Wang HMD, et al. Efficient fucoidan extraction and purification from sargassum cristae folium and preclinical dermal biological activity assessments of the purified fucoidans. *J Taiwan Inst Chem Eng*. 2022;137:104294. doi:10.1016/j.jtice.2022.104294

17. Coelho SG, Yin L, Smuda C, Mahns A, Kolbe L, Hearing VJ. Photobiological implications of melanin photoprotection after UVB-induced tanning of human skin but not UVA-induced tanning. *Pigm Cell Melanoma Res*. 2015;28(2):210–216. doi:10.1111/pcmr.12331
18. Li WR, Che X, Chen XM, Zhou ML, Luo XP, Liu T. Study of calcitriol anti-aging effects on human natural killer cells *in vitro*. *Bioengineered*. 2021;12(1):6844–6854. doi:10.1080/21655979.2021.1972076
19. Valieva Y, Ivanova E, Fayzullin A, Kurkov A, Igrunkova A. Senescence-associated β-galactosidase detection in pathology. *Diagnostics*. 2022;12 (10):2309. doi:10.3390/diagnostics12102309
20. Davalli P, Mitic T, Caporali A, Lauriola A, D'Arca DD. ROS, Cell senescence, and novel molecular mechanisms in aging and age-related diseases. *Oxid Med Cell Longev*. 2016;2016:3565127. doi:10.1155/2016/3565127
21. González-Gualda E, Baker AG, Fruk L, Muñoz-Espín D. A guide to assessing cellular senescence in vitro and in vivo. *FEBS J*. 2021;288(1):56–80. doi:10.1111/febs.15570
22. Vizioli MG, Liu T, Miller KN, et al. Mitochondria-to-nucleus retrograde signaling drives formation of cytoplasmic chromatin and inflammation in senescence. *Genes Dev*. 2020;34(5–6):428–445. doi:10.1101/gad.331272.119
23. Adewoye AB, Tampakis D, Follenzi A, Stolzing A. Multiparameter flow cytometric detection and quantification of senescent cells in vitro. *Biogerontology*. 2020;21(6):773–786. doi:10.1007/s10522-020-09893-9
24. Seebode C, Lehmann J, Emmert S. Photocarcinogenesis and skin cancer prevention strategies. *Anticancer Res*. 2016;36(3):1371–1378.
25. Krutmann J, Bouloc A, Sore G, Bernard BA, Passeron T. The skin aging exposome. *J Dermatological Sci*. 2017;85(3):152–161. doi:10.1016/j.jdermsci.2016.09.015
26. Wise LM, Inder MK, Real NC, Stuart GS, Fleming SB, Mercer AA. The vascular endothelial growth factor (VEGF)-E encoded by orf virus regulates keratinocyte proliferation and migration and promotes epidermal regeneration. *Cellular Microbiology*. 2012;14(9):1376–1390. doi:10.1111/j.1462-5822.2012.01802.x
27. Zhou Y, Zhao B, Zhang LX, et al. Combined topical and systemic administration with human adipose-derived mesenchymal stem cells (hadsc) and hadsc-derived exosomes markedly promoted cutaneous wound healing and regeneration. *Stem Cell Res Ther*. 2020;12(1):257. doi:10.1186/s13287-021-02287-9
28. Zhao B, Zhang X, Zhang Y, et al. Human exosomes accelerate cutaneous wound healing by promoting collagen synthesis in a diabetic mouse model. *Stem Cells Dev*. 2021;30(18):922–933. doi:10.1089/scd.2021.0100
29. Desrochers LM, Bordeleau F, Reinhart-King CA, Cerione RA, Antonyak MA. Microvesicles provide a mechanism for intercellular communication by embryonic stem cells during embryo implantation. *Nat Commun*. 2016;7(1). doi:10.1038/ncomms11958
30. Gurung S, Perocheau D, Touramanidou L, Baruteau J. The exosome journey: from biogenesis to uptake and intracellular signalling. *Cell Commun Signaling*. 2021;19(1). doi:10.1186/s12964-021-00730-1